Fabrication of novel AIE active chemosensor for selective detection of Pd(II) and picric acid: extended detection in HeLa cancer cell line

Susmita Das[a], Manik Das[a], Raju Biswas[b], Uttam Kumar Das[c], Soumik Laha[d], Bidhan Chandra Samanta[e], Indranil Choudhuri[f], Nandan Bhattacharya[f], Tithi Maity[a]*

[a] Department of Chemistry, Prabhat Kumar College, Contai, Purba Medinipur, West Bengal, 721404, India

[b]School of Chemical Sciences, IACS Kolkata, Kolkata, West Bengal, India

[c]Department of Chemistry, School of Physical Science, Mahatma Gandhi Central University, Bihar, India

[d]IICB, Kolkata, Jadavpur, West Bengal, India

[e]Department of Chemistry, Mugberia Gangadhar Mahavidyalaya, Purba Medinipur, India

[f]Department of Biotechnology, Panskura Banamali College, Purba Medinipur, West Bengal, India

Email: titlipkc2008@gmail.com

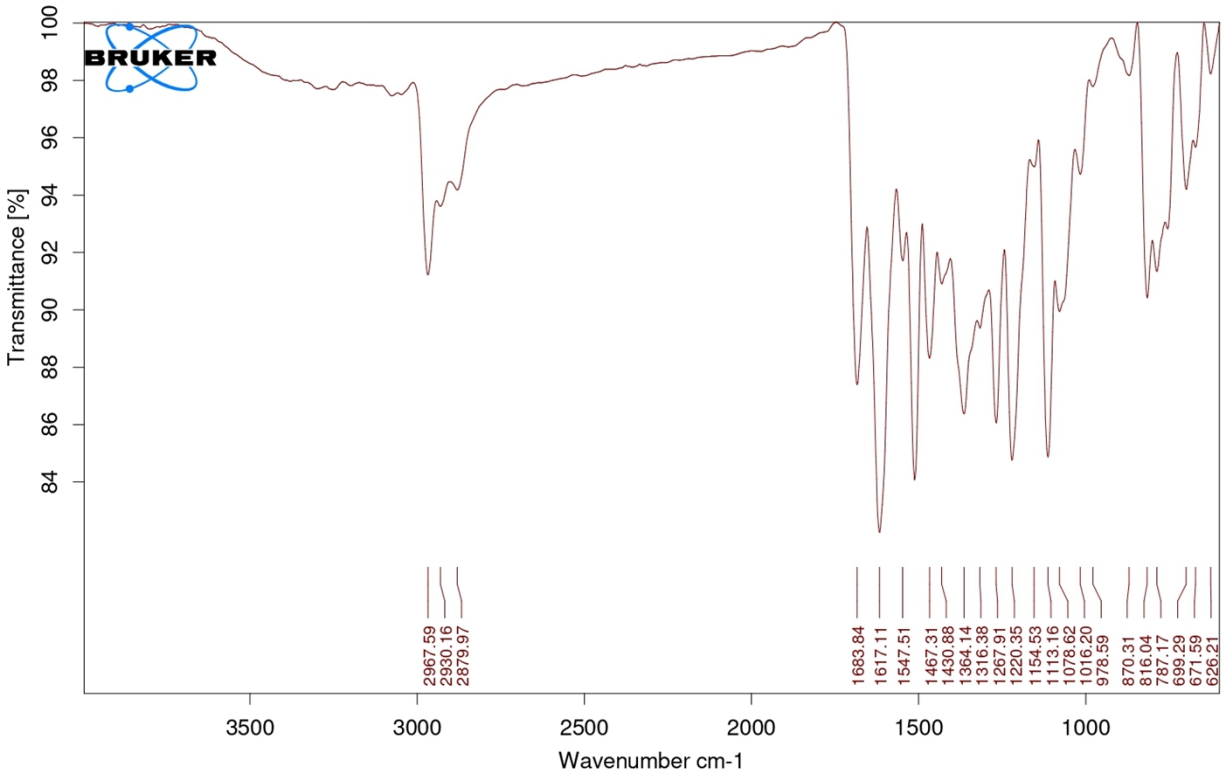

Fig. S1: FTIR spectrum **RBSB**

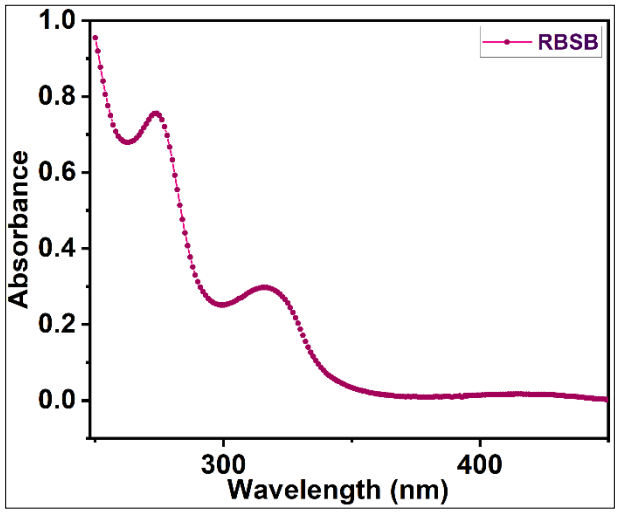

Fig. S2: UV spectrum **RBSB**

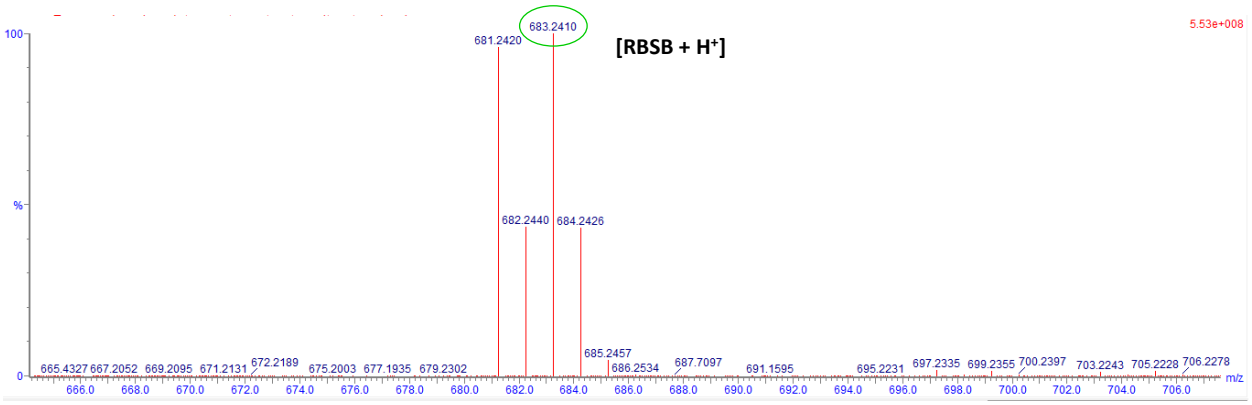

Fig. S3: Mass spectra of **RBSB**

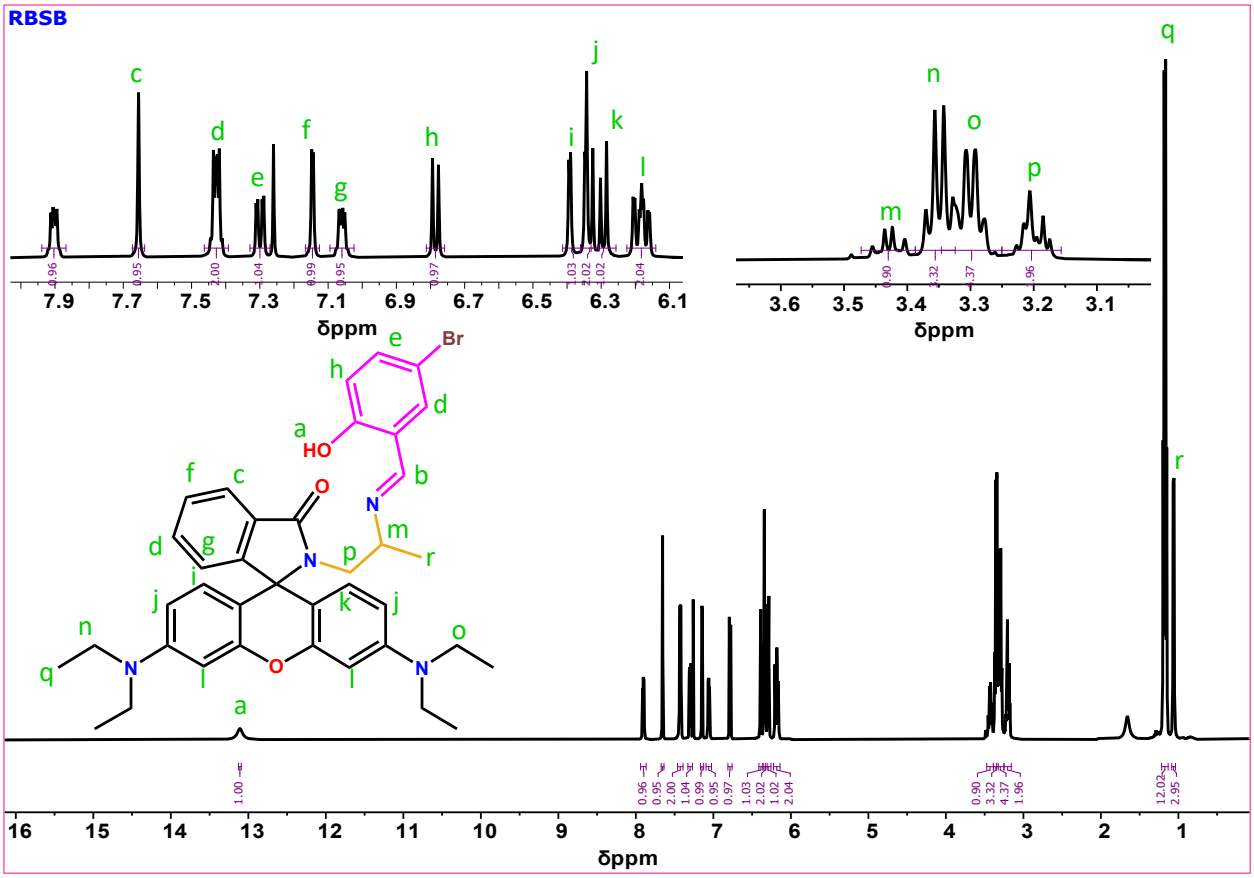

Fig. S4: ^{1}H NMR spectrum of **RBSB**

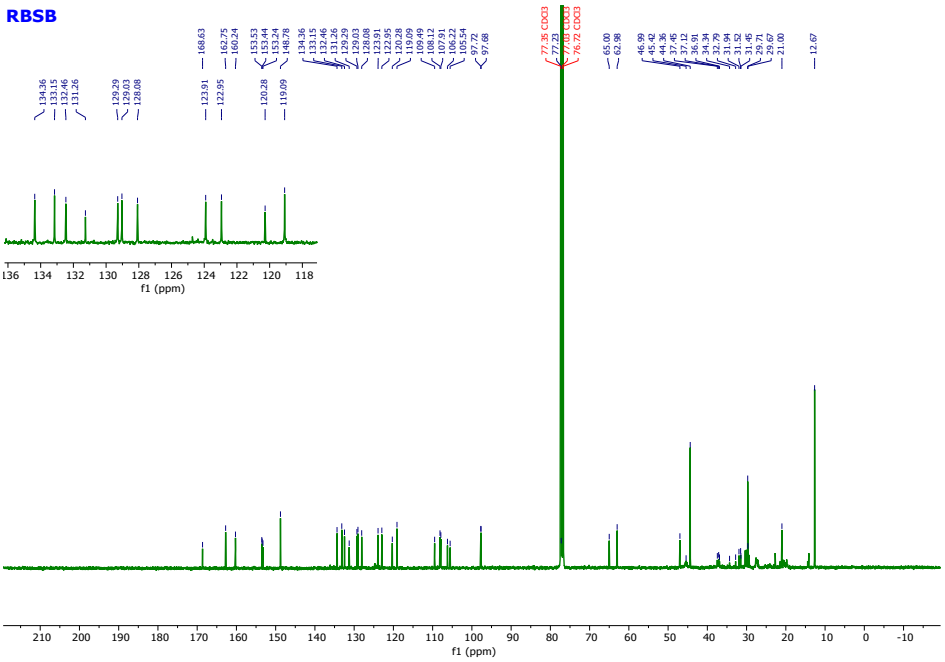

Fig. S5: 13C NMR spectrum of **RBSB**

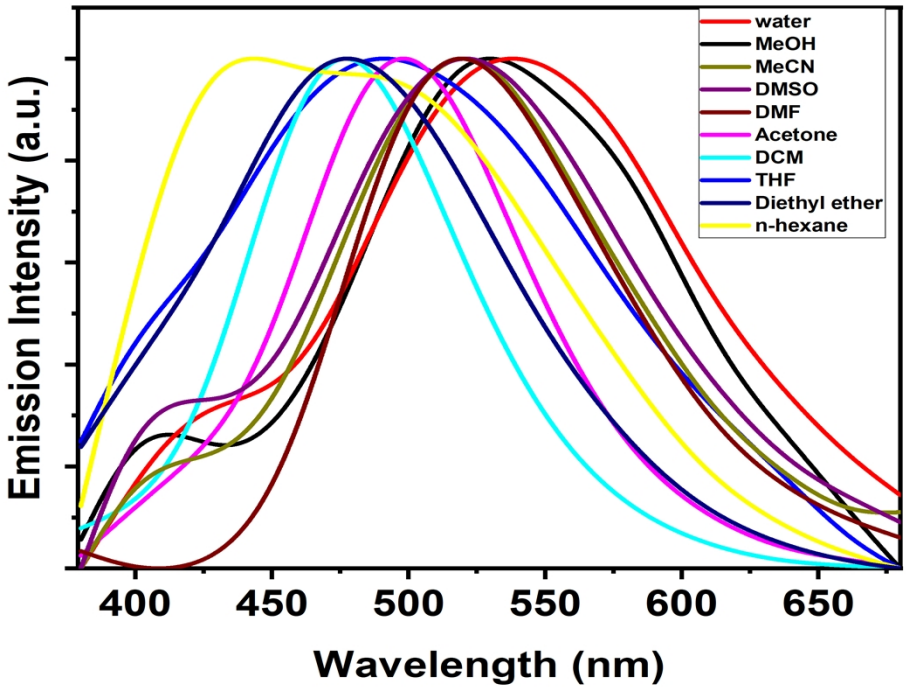

Fig. S6: Emission intensity of **RBSB** (2 μM) in different solvents with polarity difference

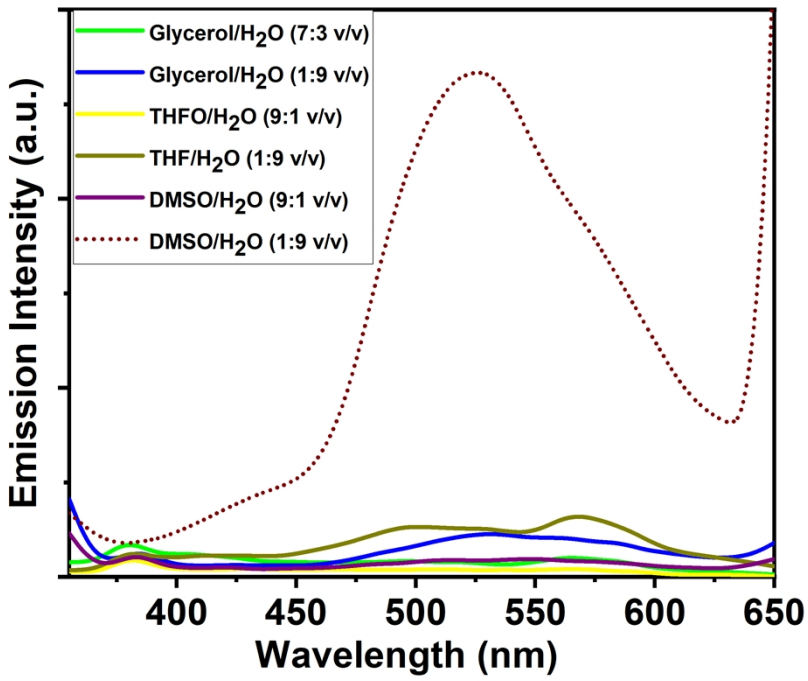

Fig. S7: The emission intensity enhancement of the probe **RBSB** in glycerol-water, THF-water, DMSO-water AIE active solvents indicating high AIE active performance in 1:9 DMSO water medium

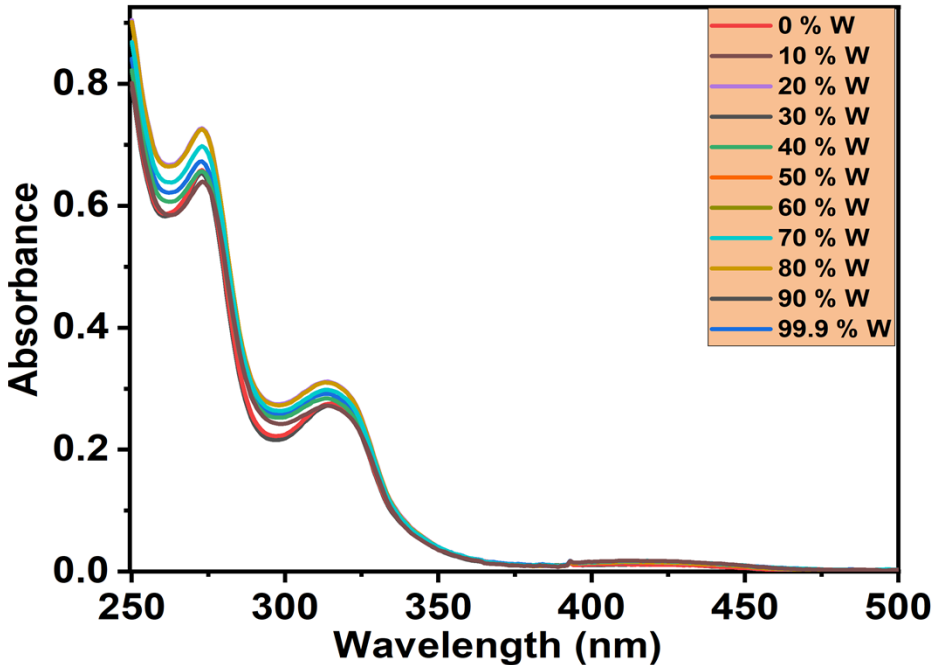

Fig. S8: Change of absorbance spectra of **RBSB** upon increasing volume percentages of water from 0% to 90% in DMSO-water AIE active medium.

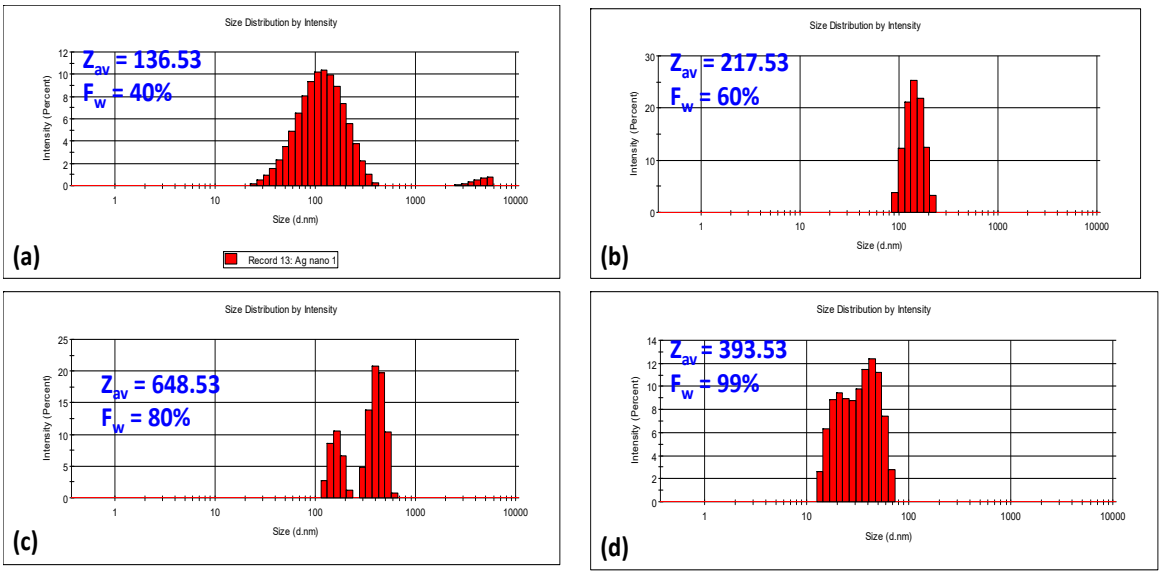

Fig. S9: Observation of the particle size change by enhancement of the water fraction with the help of DLS measurement in DMSO – H_2O medium

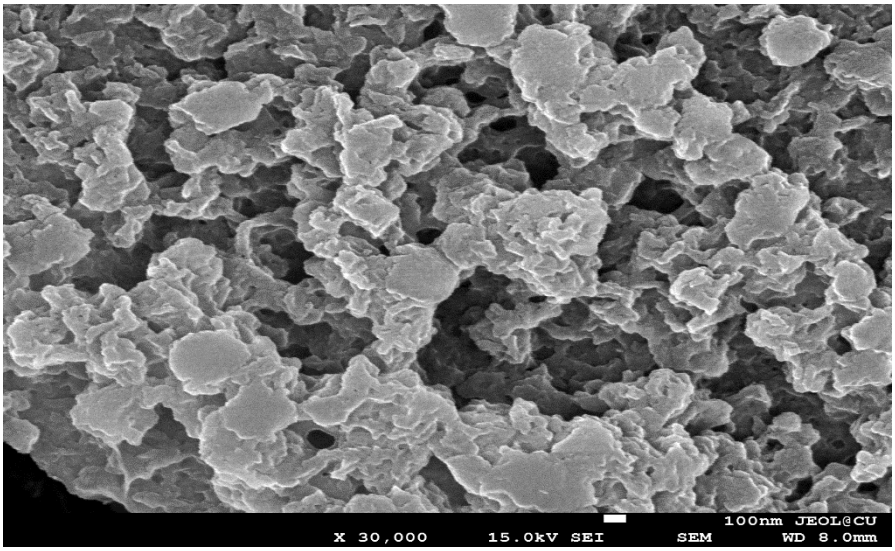

Fig. S10. SEM image of aggregated **RBSB** particle as a result of AIE behavior with a scale bar of (I) 1 mM and (II) 100 nm in DMSO – H_2O (1:9 v/v) medium

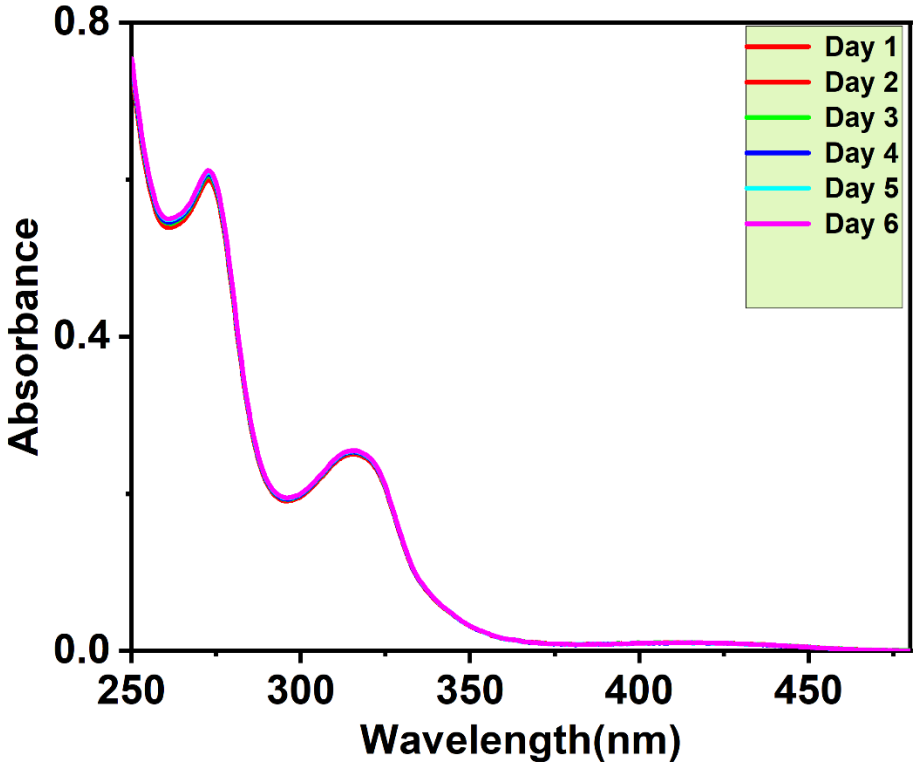

Fig. S11: Change of Absorbance of **RBSB** (2×10^{-6} M) as a function of time in DMSO – H_2O (1:9 v/v) solvent system

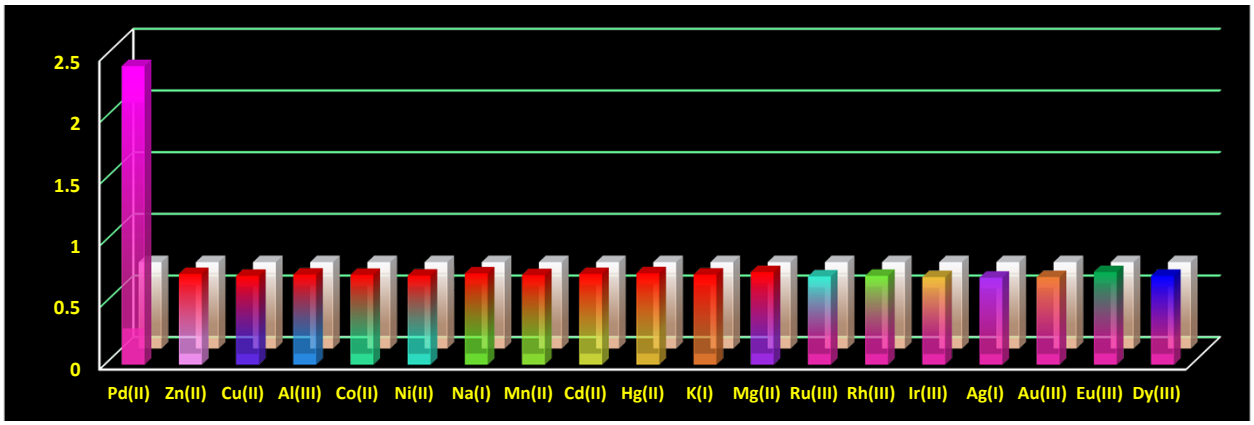

Fig. S12: Emission intensity change of **RBSB** (3×10^{-6} M) in the presence (five equivalent) of several cations including Pd(II) in DMSO-water (1:9) AIE medium over excitation at 326 nm.

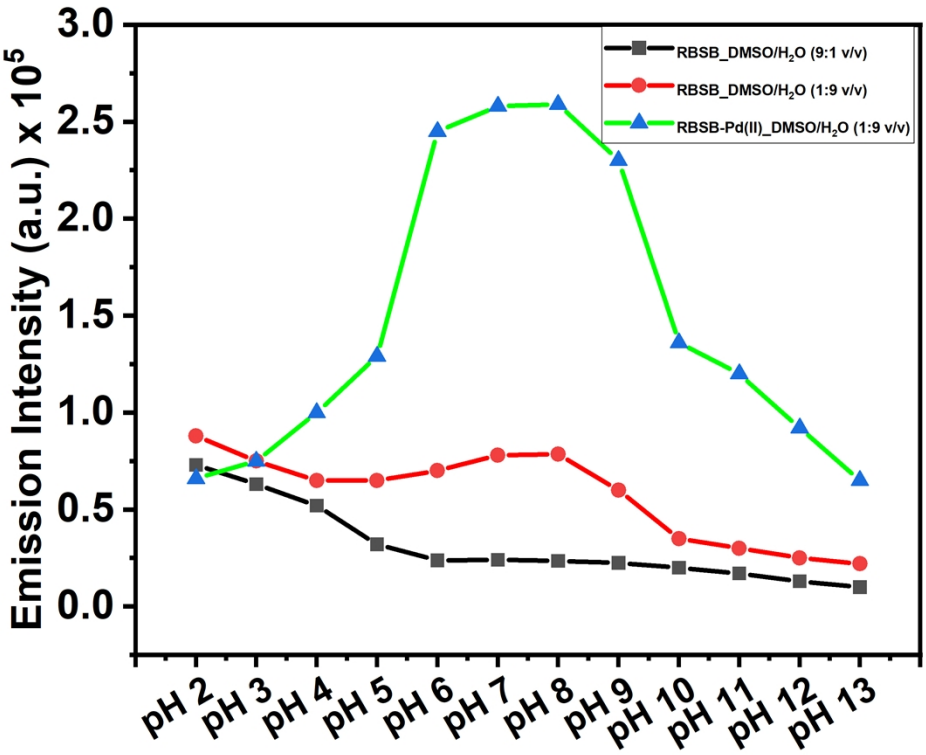

Fig. S13: Demonstration of pH effect on the emission intensity of the probe in the presence and the absence of target analyte in 9:1 DMSO-water and 1:9 DMSO water(AIE active) medium.

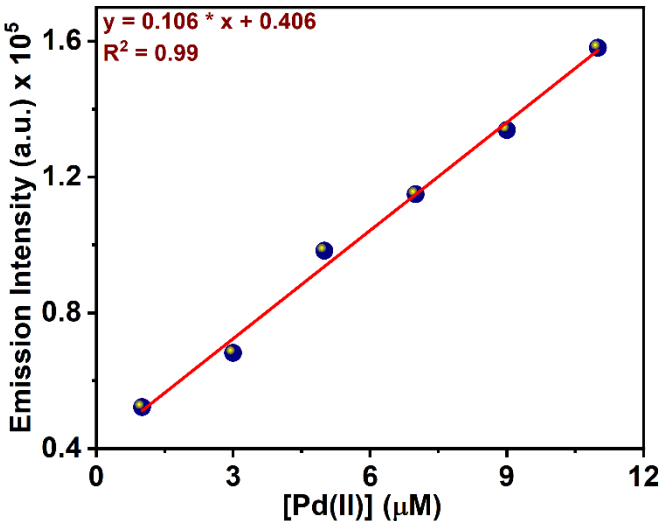

Fig. S14: Determination of LOD value during detection of Pd(II) by the probe **RBSB** in DMSO–H_2O AIE medium

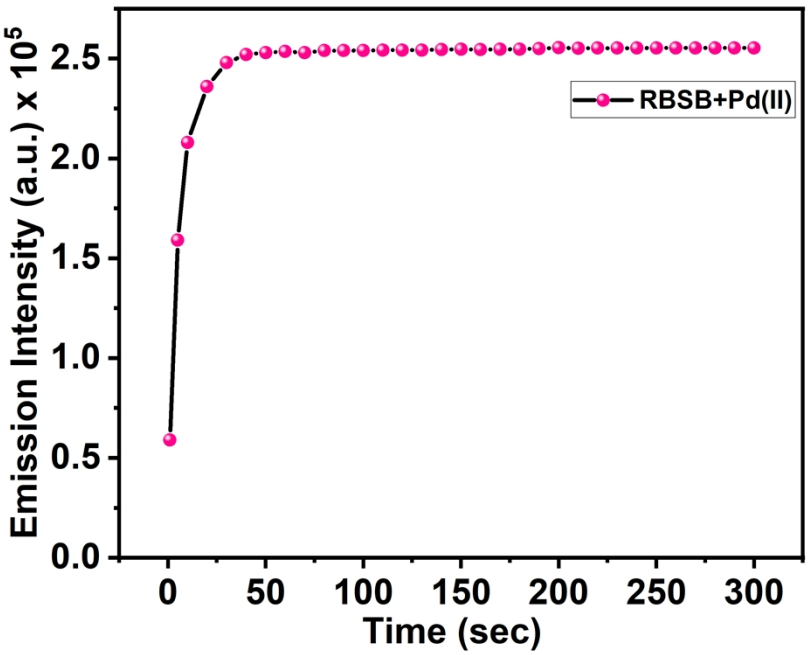

Fig. 15: Effect of response time on the emission intensity of the probe in the presence of Pd(II)

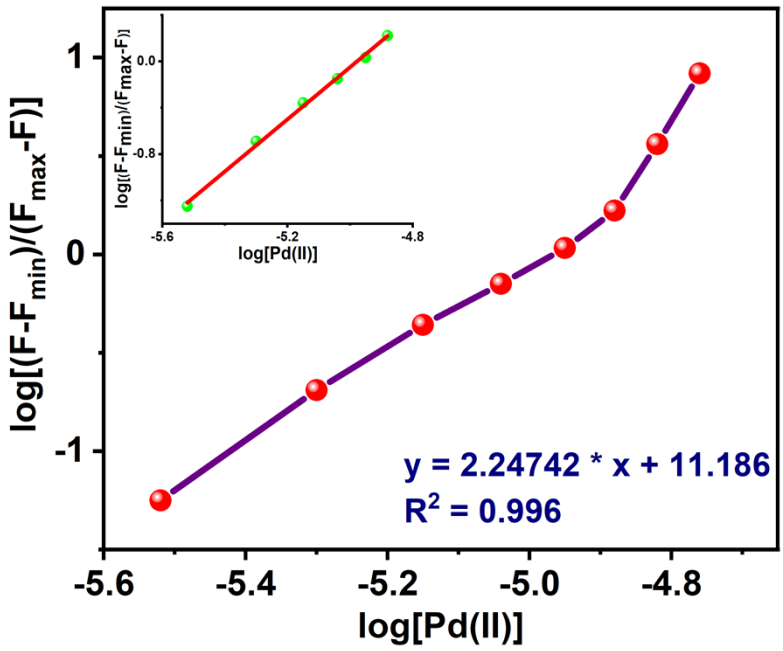

Fig. S16: Binding constant determination plot for **RBSB**-Pd(II) adduct in AIE active medium

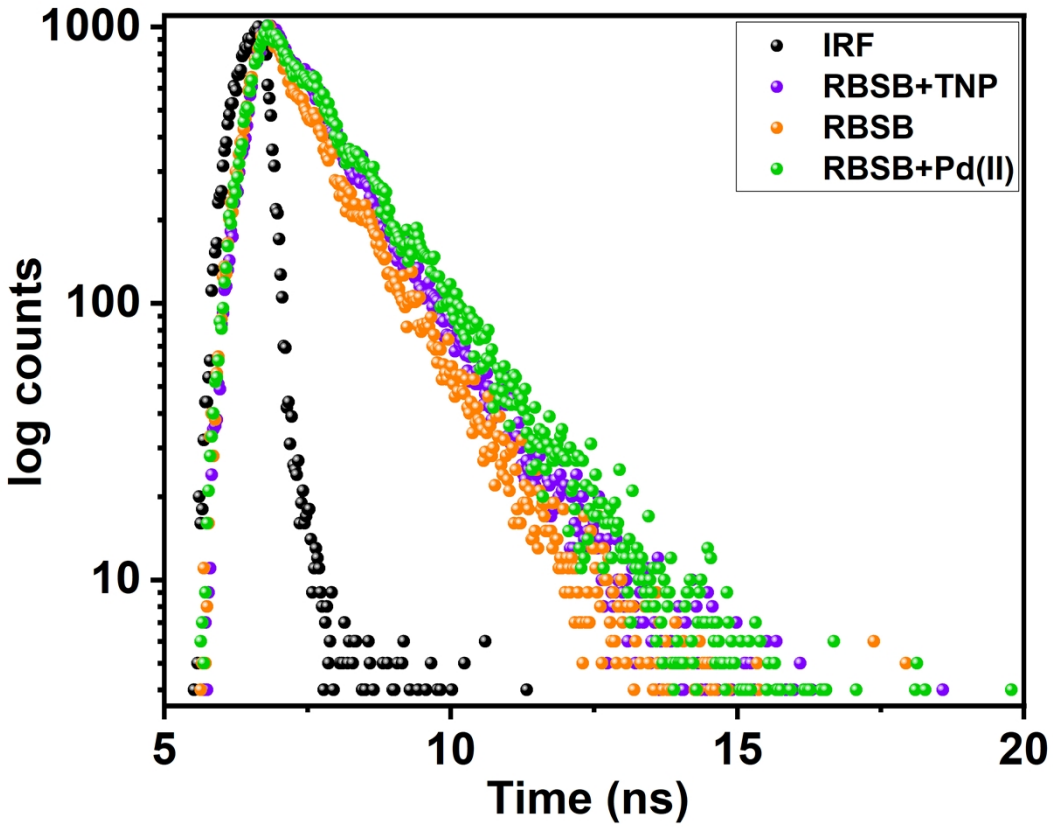

Fig. S17: Lifetime measurement of **RBSB** in the presence and the absence of Pd(II) and TNP in AIE active medium.

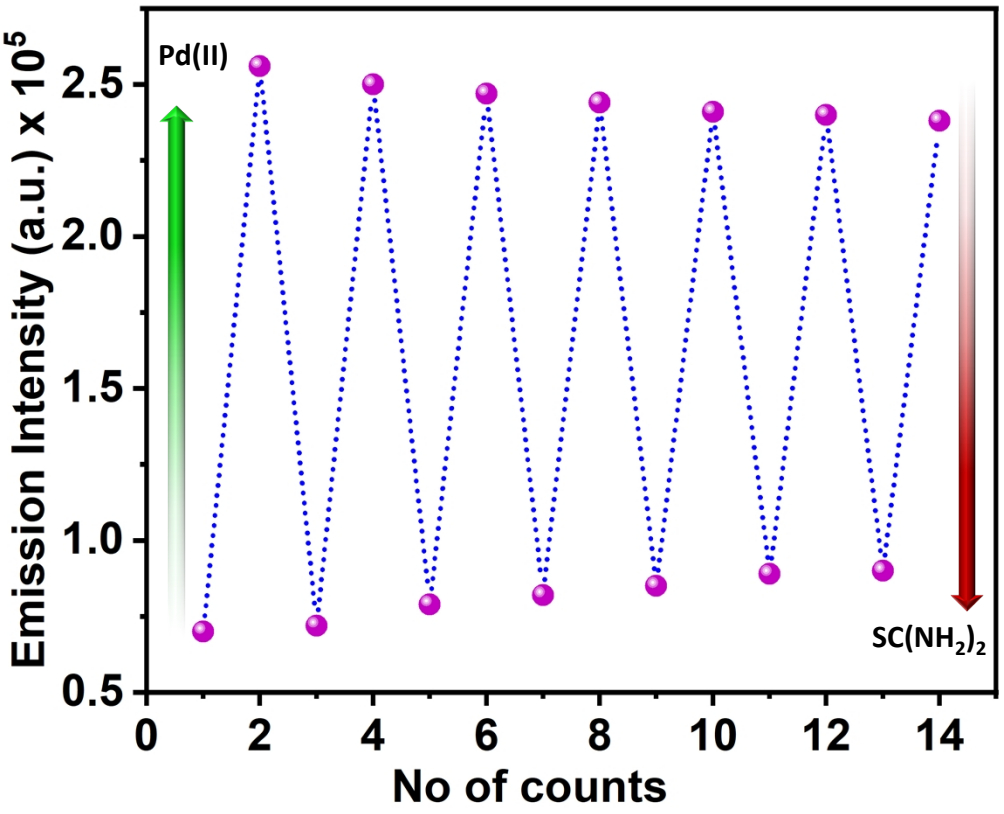

Fig. S18: The variation of fluorescence intensity of **RBSB** after alternative addition Pd(II) and thiourea, disclosing the existence of reversibility.

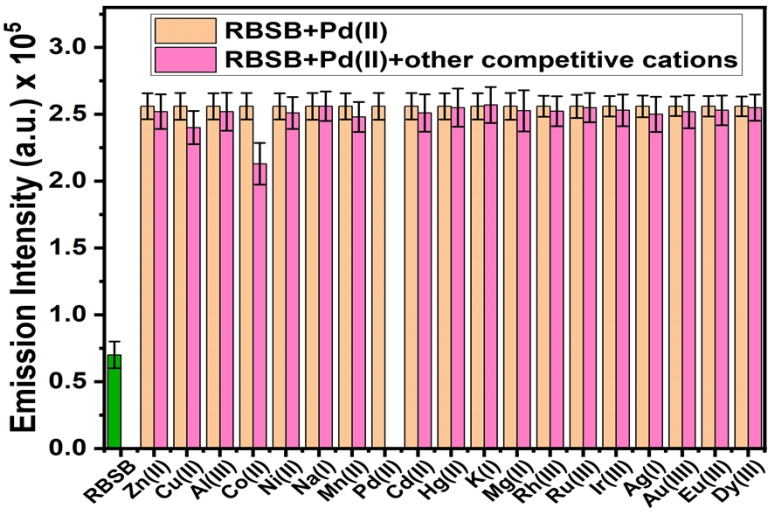

Fig. S19: Change of Emission Intensity of **RBSB** – Pd(II) adduct in the presence of several competitive metal ions to check the competitive ion effect in DMSO-water AIE active medium.

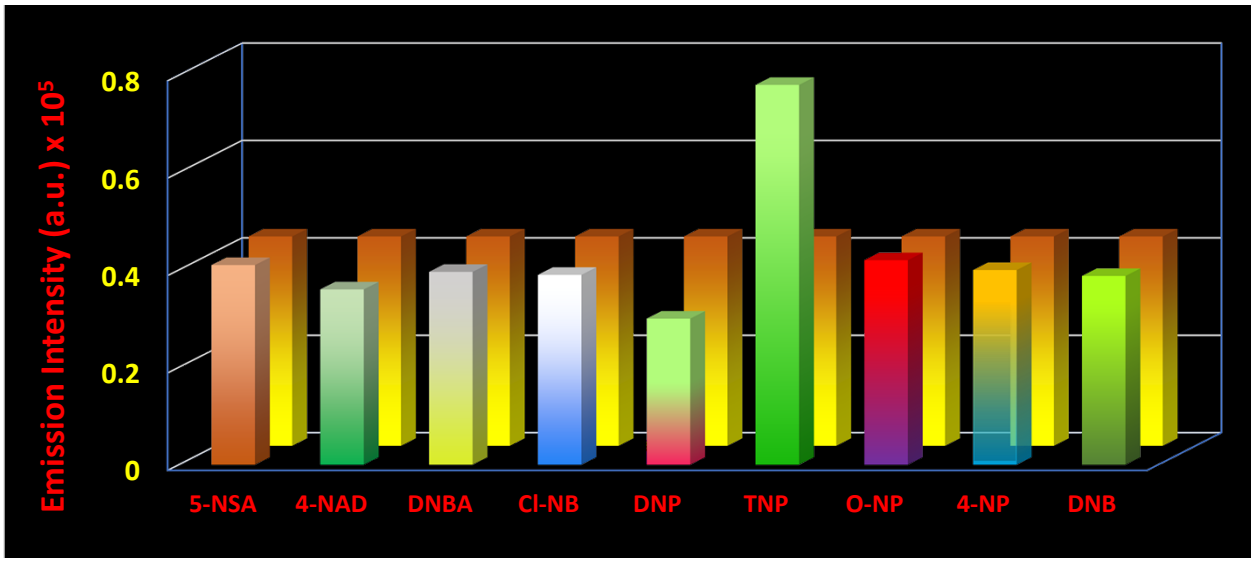

Fig. S20: Change of Emission intensity of **RBSB** (3×10^{-5} M) after separate addition of different nitroaromatic compounds (NACs) in AIE active medium

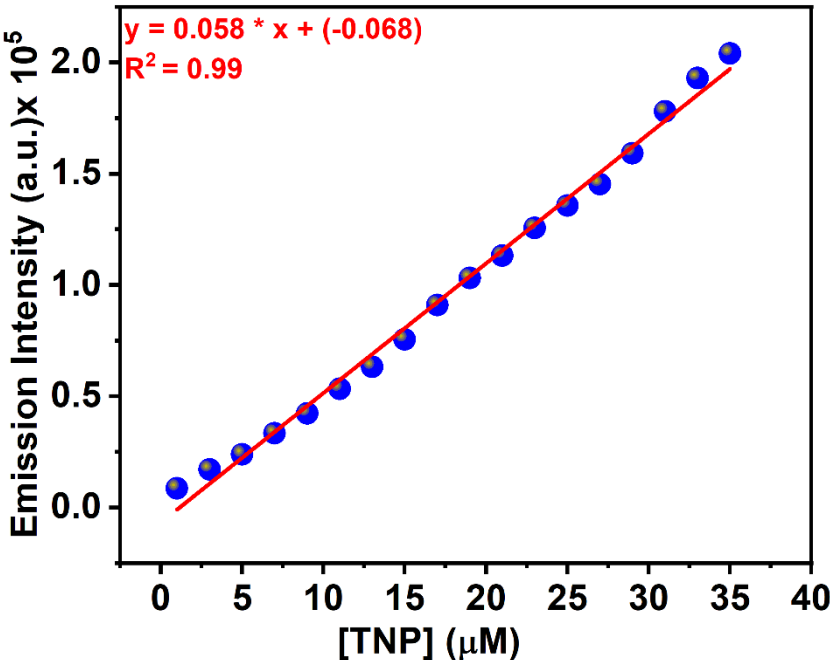

Fig. S21: Change of emission intensity of **RBSB** by the addition of PA to measure the limit of detection (LOD)

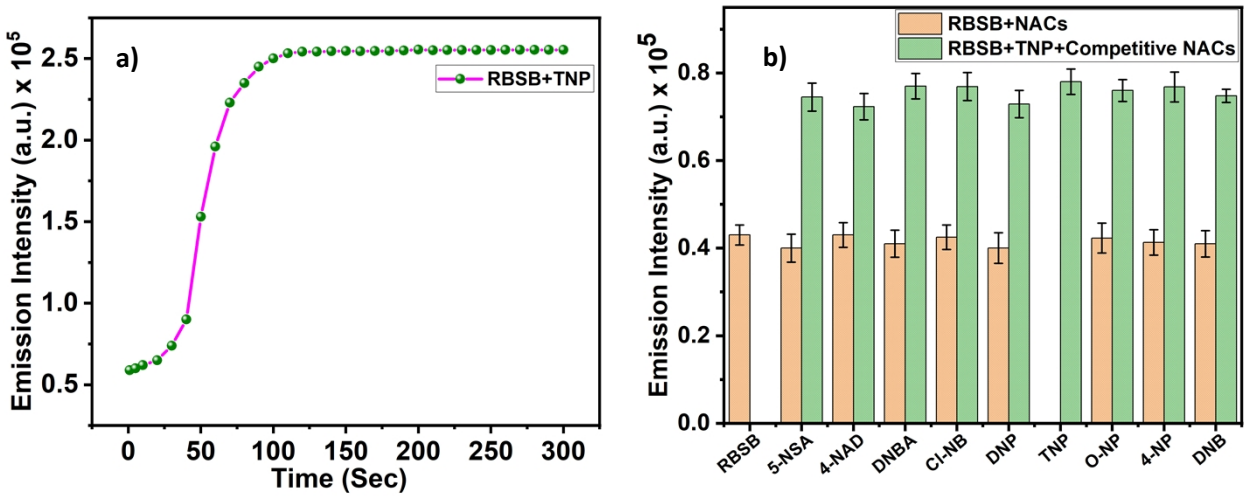

Fig. 22: a) Effect of response time on the emission intensity of the probe **RBSB** in the presence of TNP b) Emission intensity change of RBSB-TNP adduct with the presence of other individual NAC

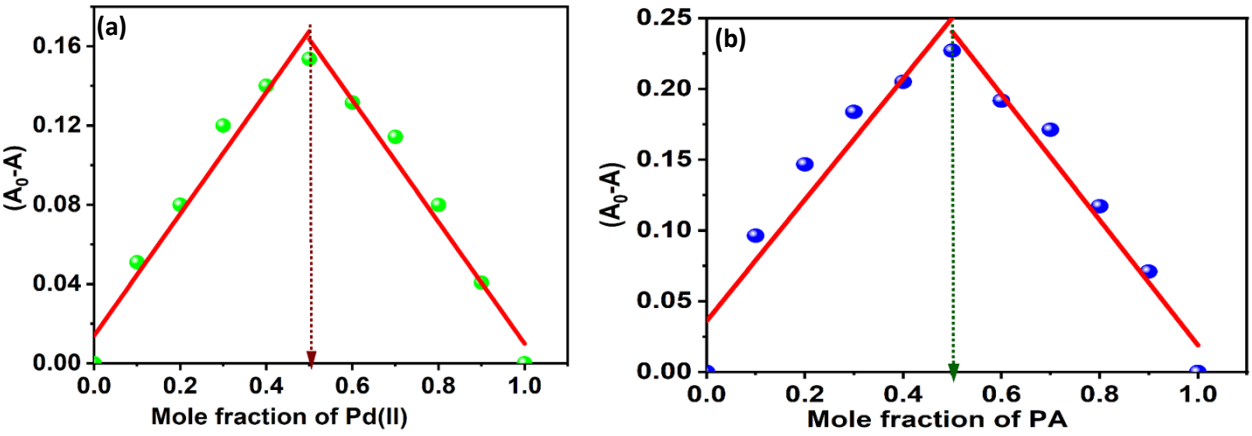

Fig. S23. Jobs plot During sensing of a) Pd(II) b) PA by **RBSB** suggesting the 1:1 probe -analyte combination

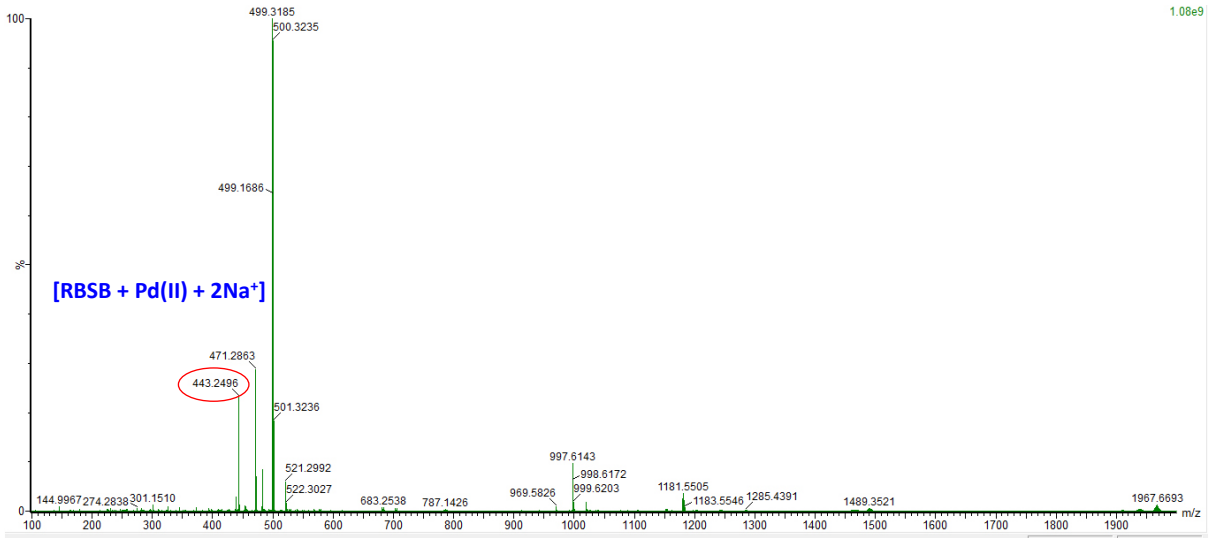

Fig. S24: Mass spectra of **RBSB** after mixing with Pd(II) in 1:1 ratio

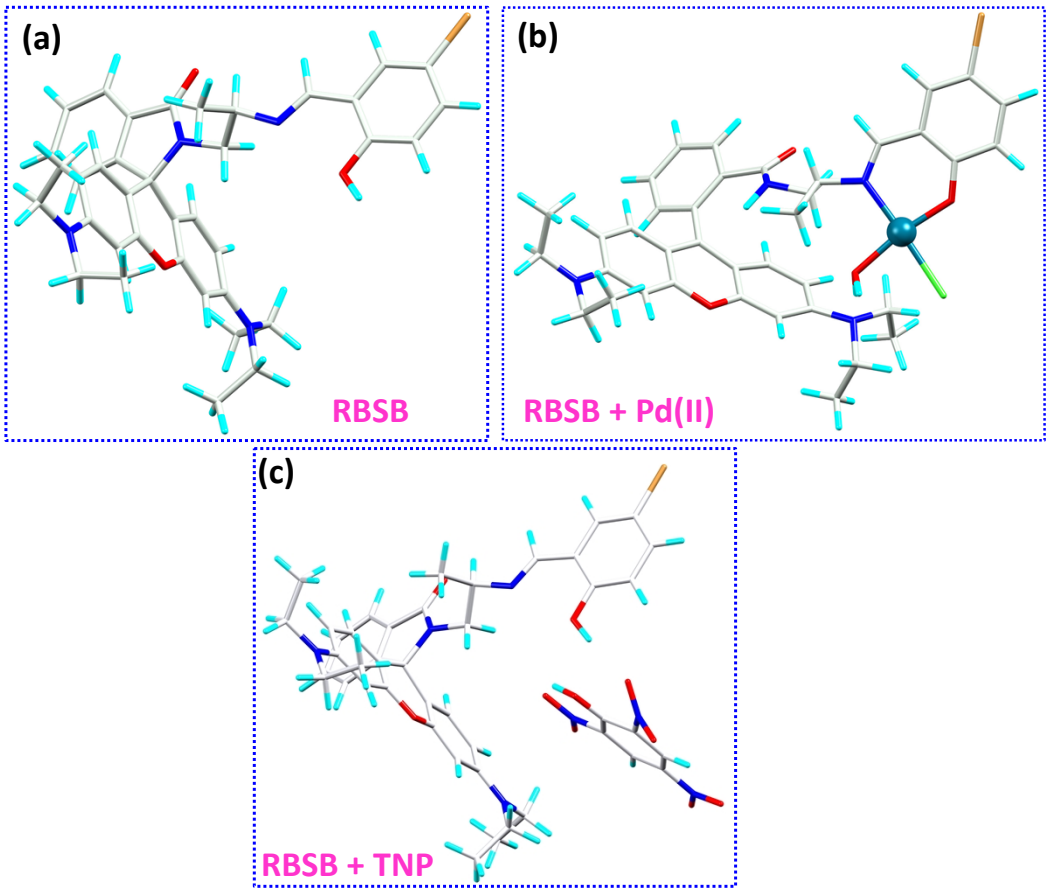

Fig. S25: The DFT optimized ground state geometry of the probe and the probe-analyte complexes.

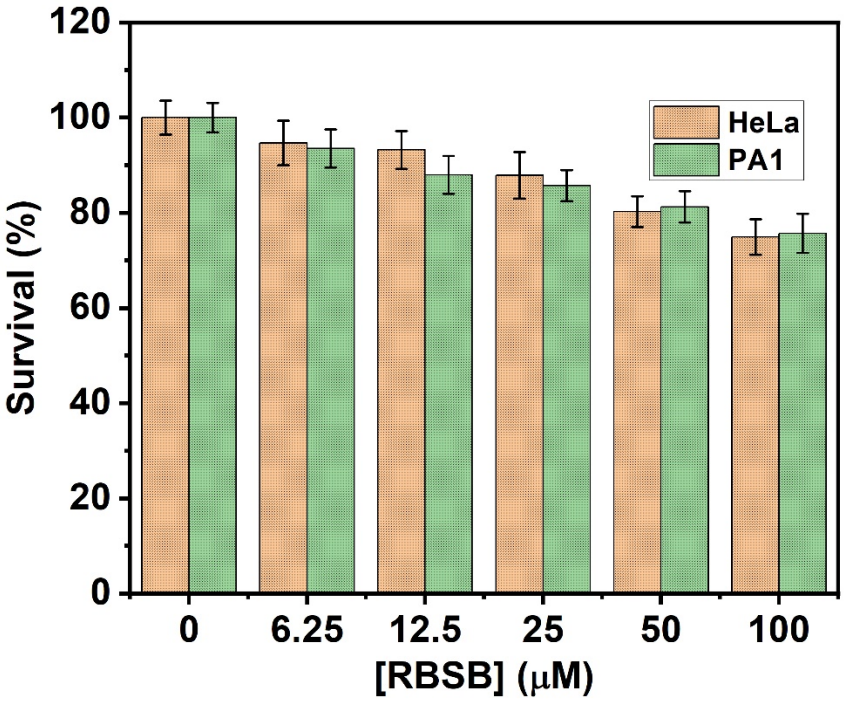

Fig. S26: Dose-dependent suppression of cell viability of **RBSB** on HeLa and PA1cell line (24 hrs)

Table S1: Intra-molecular Hydrogen bonding parameter of **RBSB**

D–H•••A	D–H (Å)	H•••A (Å)	D•••A (Å)	D–H•••A (°)	Symmetry operation for A
O1–H1•••N9	0.84	1.88	2.622(5)	147.4	x, y, z

Table S2: C-H•••O interaction parameters of **RBSB**

C–H•••O	C–H (Å)	H•••O (Å)	C•••O (Å)	C–H•••O (°)	Symmetry operation for O
C(8)–H(8)•••O34	0.95	2.46	3.307(5)	148.6	-x+1, -y+1, -z+1

Table S3: Lifetime decay parameters for **RBSB** in the presence and absence of Pd(II) in AIE active medium

sample	α_1	α_2	τ_1	τ_2	τ_{av}	χ_2	K_1	K_2
RBSB	0.58	0.42	1.94	2.90	2.34	1.00	0.171	0.344
RBSB-Pd(II)	0.44	0.56	2.08	3.79	3.03	0.995		
RBSB-TNP	0.43	0.57	2.40	3.12	2.81	0.996		

Table S4: Comparative study of literature reported probes for Pd(II) detection

Compound	**Solvent/ Sensing process**	**LOD**	**AIEE property**	**Additional analyte detection/ TNP detection**	**Application**	**Reference**
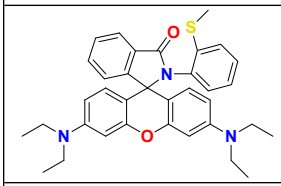	MeCN/H_2O (8:2 v/v)/ Turn on	2.4 nm	No	No/No	Paper strip	01
Al(III) MOF	H_2O/Turn off	120 nm	No	No/No	Paper strip	02
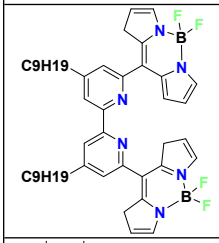	THF/ Turn off	0.97 nm	No	No/No	Paper strip, Real water, Live cell imaging	03
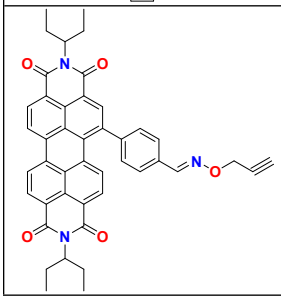	DMSO-H_2O (1:9 v/v)/ Turn off	7.90 × 10^{-8} M	Yes	Cu(II)/No	Live cell imaging, paper strip	04

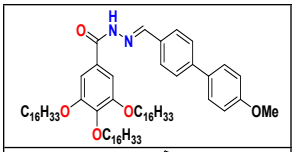	DMF/ Turn off	2.30 × 10^{-8} M	No	$H_2PO_4^-$/No	No	05
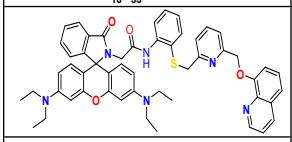	MeCN/H_2O (5:5 v/v)/ Turn on	82 nm	No	No/No	Live cell imaging	06
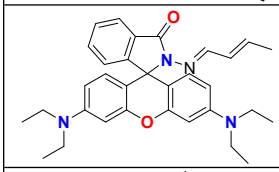	MeOH/PBS (1:1 v/v) Turn on	0.19 µM	No	No/No	Paper strip, Live cell imaging	07
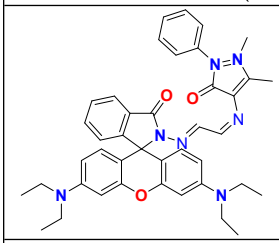	MeCN/H_2O (4:1 v/v)/ Turn on	11.9 µM	No	No/No	Live cell imaging	08
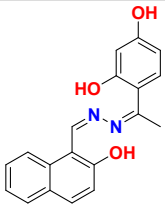	MeOH/H_2O (1:1 v/v)/	9.80 × 10^{-7} M	No	Cu(II)/No	Paper strip	09
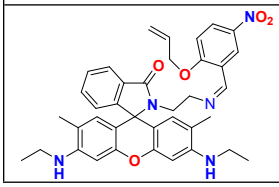	MeCN/H_2O (1:5 v/v)/ Turn on	50 nm	No	No/No	Live cell imaging	10

References

1. M. Wang, X. Liu, H. Lu, H. Wang, and Z. Qin, ACS Appl. Mater. Interfaces 2015, **7**, 2, 1284–1289.
2. P. Chakraborty, A. Rana, S. Mukherjee, and S. Biswas, Inorg. Chem. 2023, **62**, 2, 802–809.
3. F. Xu, D. Zhang, Q. Lu, R. Zhang, and J. Xia, Talanta, 2023, **253**, 123967.
4. P. Sharma, S. Kaur, S. Kaur and P. Singh, Photochem. Photobiol. Sci., 2020, **19**, 504.
5. S. Wu, H. Jiang, Y. Zhang, L. Wu, P. Jiang, N. Ding, H. Zhang, L. Zhao, F. Yin, and Q. Yang, Journal of Molecular Liquids, 2021, **327**, 114836.
6. F. K. Tang, S. M. Chan, T. Wang, C. S. Kwan, R. Huang, Z. Cai, K. and C. F. Leung, Talanta, 2020, **210**, 12063.

7. M. Yang, Y. Bai, W. Meng, Z. Cheng, N. Su, and B. Yang, Inorganic Chemistry Communications, 2014, **46**, 310–314.
8. S, Mondal, S. K. Manna, S. Pathak, A. Al Masum and S. Mukhopadhyay, New J. Chem., 2019, **43**, 3513-3519.
9. A. Kumar, Virender, B. Mohan, A. A. Solovev, M. Saini, and H. K. Sharma, Microchemical Journal, 2022, **180**, 107561.
10. A. K. Bhanja, S. Mishra, K. D. Saha and C. Sinha, Dalton Trans., 2017, **46**, 9245-9252.